NANO LETTERS

pubs.acs.org/NanoLett Letter

Metal-Enhanced Fluorescence by Bifunctional Au Nanoparticles for Highly Sensitive and Simple Detection of Proteolytic Enzyme

Jin-Ha Choi and Jeong-Woo Choi*

Cite This: https://dx.doi.org/10.1021/acs.nanolett.0c02343 Read Online

ACCESS | Metrics & More | Article Recommendations | Supporting Information

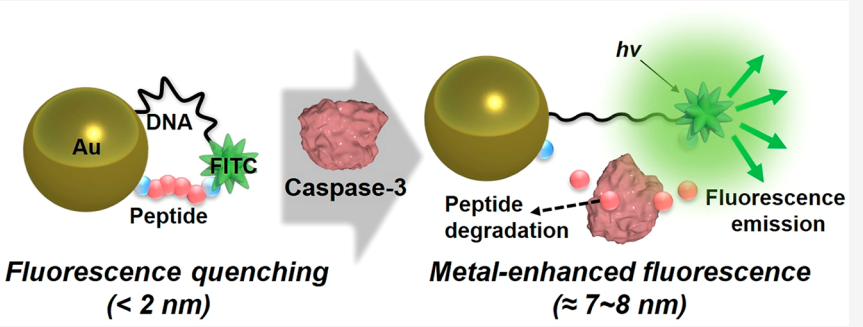

ABSTRACT: Although fluorescence-based analytical methods have been used in intracellular analyses, their sensitivity is low for the precise analysis of intracellular proteolytic enzymes to observe cell apoptosis related to cancer and neurodegenerative diseases. In this study, a metal-enhanced-fluorescence (MEF)-based highly sensitive biosensor for the detection of proteolytic enzymes is proposed for the first time by using a bifunctional Au nanoparticle (AuNP), which is connected to the fluorophore by both single-stranded DNA (ssDNA) and a peptide. Once caspase-3, a proteolytic enzyme, cuts the peptide specifically, the fluorescence signal is drastically increased because the ssDNA maintains an optimal distance for the MEF. The proposed sensing method shows the highly sensitive detection of caspase-3 based on just a simple enzymatic cleavage reaction within 1 h, and caspase-3-related preapoptotic cell detection was successfully carried out with high sensitivity. The proposed sensing method is a rapid, simple, and one-step technique for the real-time monitoring of intracellular proteolytic enzymes and can be applied to the early diagnosis of cancer and neurodegenerative diseases.

KEYWORDS: *Metal-enhanced fluorescence (MEF), Caspase-3, Au nanoparticle (AuNP), Nanobiosensor, Proteolytic enzyme*

Proteolytic enzymes, which degrade specific proteins, have played an important role in the living system, from the biomolecular to the organ level.[1,2] For instance, matrix metalloproteinases (MMPs) degrade both matrix and non-matrix proteins in the extracellular environment of cells and are involved in the activation/inactivation of several biomolecules by the cleavage of cell surface receptors, the release of apoptotic ligands, and so forth.[3−5] Some proteolytic enzymes have different expression levels based on the physiological conditions of hosts and organs. Typically, the concentration of the MMPs is relatively high in the case of the cancerous state because they are utilized on the angiogenesis of tumor sites for nutrient and oxygen supply.[3,6,7] In this respect, proteolytic enzymes have been widely used as biomarkers for the diagnosis of some specific diseases such as cancers, neurodegenerative diseases, and other biological reactions.[8−12] To detect proteolytic biomarkers selectively, most of the proteolysis-based biosensors have exploited specific peptide sequences consisting of fewer than 10 amino acids that could be cleaved by particular proteolytic enzymes such as MMPs,[13−15] the caspase family,[16−18] and prostate-specific antigens (PSAs).[19−21] Using specific sequences can be done to measure in a very selective manner, similar to an immunoassay.

For the successful detection of proteolytic enzymes, diverse analytical methods have been applied to convert the detection to a signal such as fluorescence resonance energy transfer (FRET),[18,22] optical analysis,[23,24] and electrochemical analysis.[25,26] Among them, the FRET-based biosensing system has been extensively studied using a distance-dependent change in fluorescence intensity. In the FRET system, the acceptor hampers the fluorescence emission from the donor when they are located close to each other via the peptide strand as a bridge. If the distance increases because of the proteolytic cleavage reaction of the enzyme, then the fluorescence

Received: June 5, 2020
Revised: August 18, 2020
Published: August 18, 2020

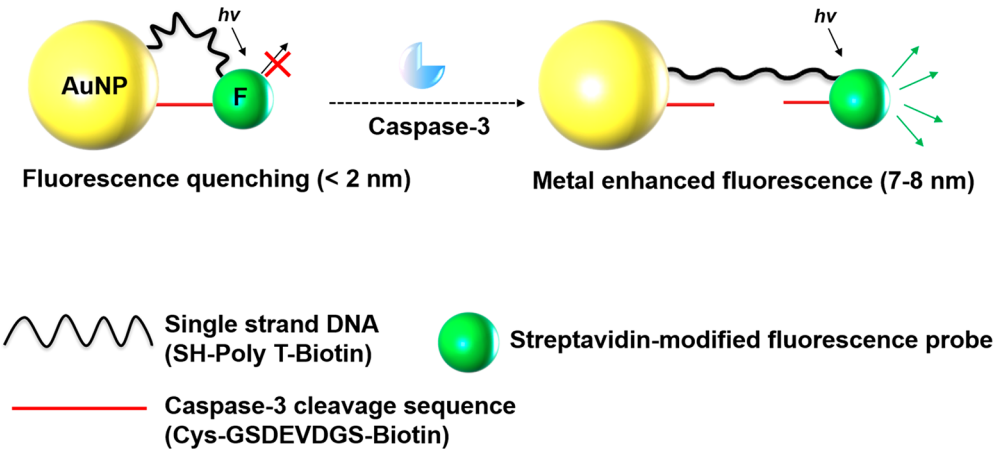

Figure 1. Schematic diagram of the MEF-based caspase-3 biosensor. Before the cleavage reaction, Au nanoparticles (AuNPs) and FITC are closely positioned via a peptide strand. After the reaction with caspase-3, the distance between the AuNP and FITC increases, and the metal-enhanced fluorescence occurs as ssDNA maintains a constant distance.

intensity of the donor increases, whereas the acceptor signal weakens. The change in the fluorescence signal facilitates a readout of the activity or concentration of proteolytic biomarkers. By using this fluorescence-based analytical system, several proteolytic enzymes have been effectively measured with specific nanomaterials such as carbon-based nanomaterials (carbon nanotube[27] and reduced graphene oxide[28]), metal nanomaterials (Au, Ag),[29,30] and fluorescent nanomaterials (quantum dot,[31] upconversion nanoparticles[32]). Target proteolytic enzymes could be simply detected in a short time because of the absence of the labeling process for signal generation compared with the conventional immunoassay, which can be sensitive and selective in detection but has some drawbacks such as the time commitment, the difficulty in maintaining its activity and stability, and the high price of antibodies. In the case of FRET, however, the signal intensity can be somewhat low because of the low energy transfer efficiency during the FRET phenomenon compared with other analytical methods. It can have an adverse effect on sensitive detection, even though it enables the rapid, user-friendly, and straightforward analysis of proteolytic enzymes. Thus there is an urgent need to develop novel systems that can improve the sensitivity in a stable, fast, and simple manner.

Metal-enhanced fluorescence (MEF) is one of the emerging detection approaches. It involves amplification of the fluorescence intensity when fluorescent molecules are positioned near a noble-metal nanostructure; here the emission intensity can be drastically enhanced.[33,34] Localized surface plasmon resonance (LSPR) of the noble metal can strongly magnify the absorption of the incident light.[35] The energy can be transferred to the fluorescent molecules if the LSPR band has a significant overlap with the excitation or emission spectrum of the molecules with an optimal distance from the metal to a fluorophore. On the contrary, the strong electromagnetic field generated by the LSPR phenomenon can quench the fluorescence emission when the distance from the metal surface is very small (<2 nm). Therefore, controlling the distance is essential to take advantage of inducing the MEF phenomenon. In our previous studies, the MEF-based exosomal miRNA biosensor and the cell-free DNA (cfDNA) detection system were presented with high sensitivity.[36,37] Similar to our nucleic acid detection system, the distance can be changed by the activity or concentration of the target proteolytic enzymes.

In this study, for the first time, we developed a novel proteolytic enzyme nanobiosensor that consists of Au nanoparticles (AuNPs) and a specific peptide sequence (DEVD)[38] that is recognized and cleaved by caspase-3, which is closely related to apoptotic cells and the diagnosis of cancers and neurodegenerative diseases.[16−18] In this system, a double bridge between the AuNP and fluorescein isothiocyanate (FITC) was created by the peptide and single-stranded DNA (ssDNA), and the fluorescence signal was quenched because of the short length of the peptide. The peptide could be selectively degraded, and the distance was increased. ssDNA was utilized to maintain the distance between Au and the FITC after the peptide cleavage reaction. The FITC−ssDNA−AuNP emitted an enhanced fluorescence signal compared with the original fluorescence signal from FITC due to the optimal distance of MEF around 7 to 8 nm. Comparing other conventional immunoassay-based enzymatic biosensors, this AuNP-based sensing system required just a simple proteolytic cleavage reaction in a rapid and highly sensitive manner. Using this one-step detection system, caspase-3 was measured both in the cell-free configuration and under intracellular circumstances with enhanced sensitivity by the MEF effect to recognize preapoptotic cells.

RESULTS AND DISCUSSION

Characterization of the Bifunctional AuNP. A nanoscale MEF-based detection system for the caspase-3 measurement was developed using a 30 nm sized colloidal bifunctional AuNP containing a small peptide strand, ssDNA, and streptavidin−FITC molecules (Figure 1). The small peptide strand and ssDNA were modified by cysteine and thiol groups, which were easily attached to the Au surface by a Au−thiol interaction. In addition, the peptide strand and ssDNA were also tagged to biotin, which was bound to the streptavidin−FITC molecule at the other side. In the quenching state (left in Figure 1), streptavidin−FITC molecules were positioned close to the surface of the AuNP (<2 nm) because the length of the nine amino acids and biotin (CGSDVEDGS-biotin) was ∼1.5 nm. Thus FITC could not emit its fluorescence at 520 nm. When caspase-3 degraded the specific peptide sequence (DEVD), bridging between the AuNP and FITC, the

https://dx.doi.org/10.1021/acs.nanolett.0c02343
Nano Lett. XXXX, XXX, XXX−XXX

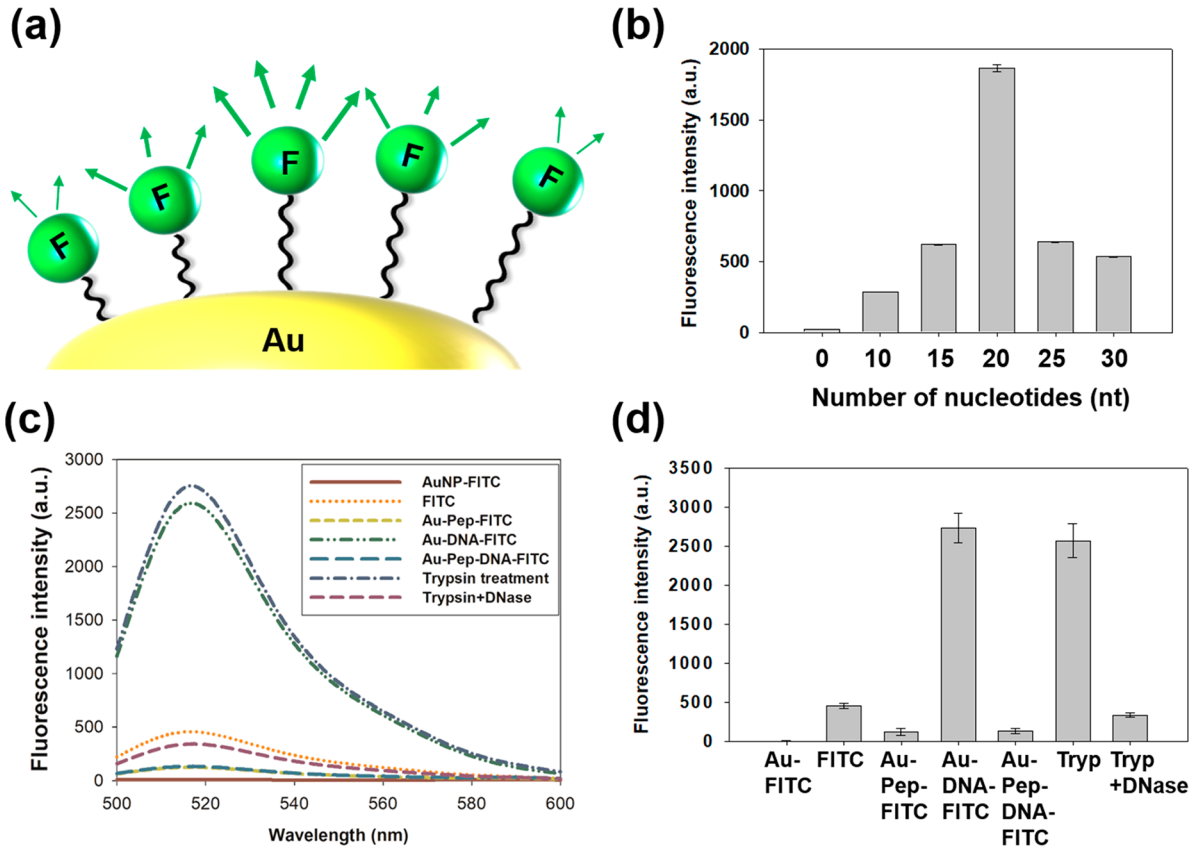

Figure 2. Confirmation of the MEF phenomena using bifunctional AuNP. (a) Schematic diagram of the MEF depending on the length of the ssDNA, which decides the distance between the AuNP and FITC. (b) Fluorescence intensity of the bifunctional AuNPs depending on the length of the ssDNA. (c) Fluorescence spectrum of the AuNP−FITC, FITC, AuNP−peptide−FITC, AuNP−DNA−FITC, as well as AuNP−peptide−DNA−FITC after trypsin treatment, and trypsin+DNase treatment. (d) Fluorescence intensity of the bifunctional AuNP at 520 nm, corresponding to panel c.

fluorescence emission of FITC was enhanced by the MEF phenomenon with around 7 to 8 nm distance[39] through the bound ssDNA (poly T, 20 base pairs), whose length was maintained through caspase-3 cleavage of the peptide bridge. To validate the functionalization of AuNPs, as a first step, the protein corona structure on AuNPs was confirmed by transmission electron microscopy (TEM) in Supplementary Figure 1a. We speculated that the short peptide strand and streptavidin connected by the biotinylated peptide could be found in TEM images by the negative staining method. In addition, it is possible to directly verify the linkage of the AuNP, ssDNA, peptide, and streptavidin systematically. Supplementary Figure 1b exhibits the UV−vis absorbance spectrum for each nanomaterial (AuNP, AuNP−ssDNA, AuNP−peptide, AuNP−ssDNA−peptide, and AuNP−ssDNA−peptide−streptavidin) for the verification of the functionalization of AuNPs through the absorbance peak shift. The bare AuNP had a specific single absorbance peak at 526.2 nm. This peak could be shifted to the longer wavelength after some biomaterials were attached to the surface of the AuNP because of the LSPR effect.[40,41] Typically, the red-shifted peak phenomena of noble nanoparticles, including AuNPs, depended on the nanoparticle size, particle aggregation, and local dielectric environments, which affect the surface plasmon resonance phenomena. This absorbance method was appropriate for directly recognizing binding events between biomolecules and nanoparticles. As shown in Figure 1b, the absorbance peak of the bare AuNP was at 526.2 nm, whereas the peak for the bifunctional AuNP was gradually shifted to the right by ∼1 nm. Therefore, the linkage of the ssDNA, peptide, and streptavidin to the AuNPs was successfully demonstrated by a change in the absorbance peak. Besides these analytical methods, the confirmation of the bifunctional AuNP was assessed by the bicinchoninic acid (BCA) assay and ssDNA quantification kit (Supplementary Figure 2). In the BCA method, proteins induce the reduction of Cu(II) cations to Cu(I). Bicinchoninic acid is then added, and the resultant colorimetric change is assessed. The peptide concentration in the bifunctional AuNP solution was 10 μM, and its absorbance at 562 nm was ∼0.38 (Supplementary Figure 2a). The peptide concentration in the supernatant after attachment to the AuNP surface was ∼1 μM, corresponding to the absorbance value (0.22). These results clearly indicate strong peptide attachment (∼90% of the applied peptide) to the AuNPs. In the case of the ssDNA attachment on AuNPs, a similar method was applied using the Qubit ssDNA assay kit (Supplementary Figure 2b). We estimated 73% of the 10 μM ssDNA to be attached to AuNPs through a similar method to the peptide quantification.

Confirmation of the MEF Phenomenon by the Bifunctional AuNP. In this study, MEF is the central mechanism of improvement in sensitivity. Thus it is critical to optimize the fluorescence-enhancing effect proportional to the caspase-3 concentration. The fluorescence signal amplification depends on the particle size and shape, the absorbance wavelength, the distance between the metal and the

https://dx.doi.org/10.1021/acs.nanolett.0c02343
Nano Lett. XXXX, XXX, XXX−XXX

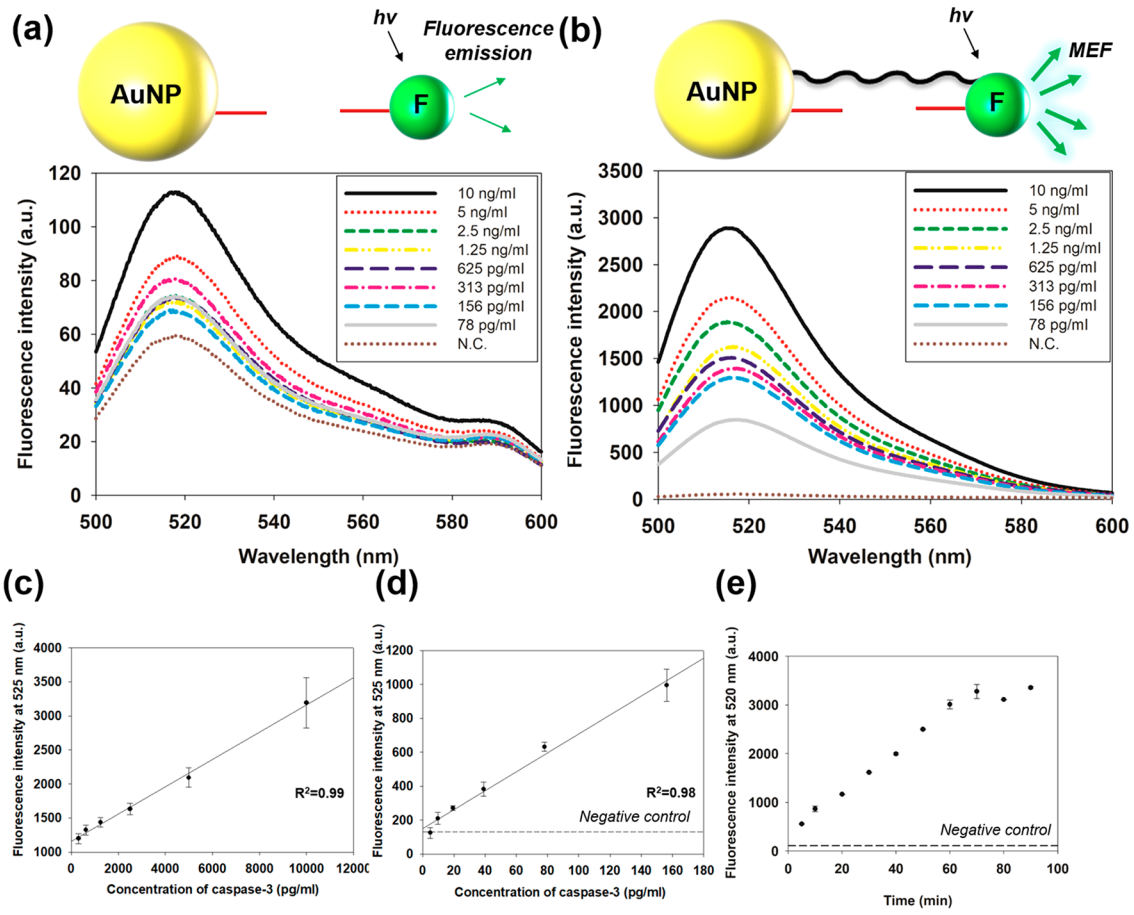

Figure 3. Measurement of caspase-3 using an MEF-based bifunctional AuNP biosensor. (a) Fluorescence spectrum of the bifunctional Au nanoparticle without ssDNA after caspase-3-mediated proteolytic reactions. (b) Fluorescence spectrum of the bifunctional Au nanoparticle with ssDNA after caspase-3-mediated proteolytic reactions. (c,d) Linear curve of the fluorescence intensity at 520 nm according to the concentration of caspase-3 from 10 pg/mL to 10 ng/mL. (e) Fluorescence intensities of the enzymatic kinetics bifunctional Au nanoparticle without ssDNA with 10 pg/mL caspase-3 over time.

fluorophore, and so on. Among them, the distance is the dominant factor for the drastic change in fluorescence because noble metals also have a quenching effect when the distance is <5 nm. A sudden change in fluorescence intensity can result in the sensitive detection of the proteolytic target, including caspase-3. Therefore, the extent of the enhancing effect was examined by using several lengths of bridging ssDNA depending on the number of thymine bases (from 0 to 30; Figure 2a,b). As a result, 20 nucleotides (NTs) of ssDNA, whose length was ~7 nm, confirmed the optimal distance between the AuNP and FITC for inducing an efficient MEF phenomenon. Moreover, it was confirmed that the degradation of the peptide bridge resulted in fluorescence enhancement with the ssDNA bridge by applying trypsin, which could degrade the peptide at random (Figure 2c,d). Besides the trypsin reaction, many cases of functionalized AuNPs were tested to understand the MEF phenomenon using these bifunctional AuNPs. Four groups could be classified from the fluorescence intensity. First, AuNPs with FITC could not emit fluorescence because the distance was very short. The second groups, which are AuNP−peptide−FITC and AuNP−ssDNA−peptide−FITC, also had a little fluorescence emission because of its distance decided by peptide length, which was still short. Third, FITC molecules displayed their original fluorescence intensity. Similarly, applying trypsin and DNase to the bifunctional AuNPs resulted in fluorescence intensity higher than those of the second group because FITC was away from the surface of the AuNP due to the disconnected ssDNA/peptide and AuNP. Lastly, bifunctional AuNPs composed of DNA and FITC without a peptide exhibited the highest emission values by the MEF phenomenon. A comparison of the FITC molecules showed that the intensities of MEF-inducing bifunctional AuNPs increased by about seven times.

Ultrasensitive Detection of Caspase-3 through the Change of Fluorescence Intensity from Quenching to MEF State. The detection of caspase-3 using its proteolytic property was accomplished using specific peptide and ssDNA-functionalized AuNPs by generating MEF phenomena. In this sensing system, AuNPs were utilized in dual roles: a fluorescence quencher and enhancer. In general, AuNPs are known to have a superior quenching efficiency over a broad range of wavelengths compared with other organic quenchers and an excellent fluorescence-enhancing effect. Therefore, the AuNP concentration should be optimized for the amplification of fluorescence intensity. We had tested diverse concentrations of AuNPs, and 2×10^{11}/mL showed the most amplified fluorescence signal (Supplementary Figure 3). A low concentration of AuNPs exhibited weak fluorescence emission due to the small amount of FITC, whereas a high concentration showed a dominant quenching effect due to the closer distance between AuNPs. As mentioned in previous section, ssDNA played a very important role in enhancing the

https://dx.doi.org/10.1021/acs.nanolett.0c02343
Nano Lett. XXXX, XXX, XXX−XXX

Table 1. Limit of Detection (LOD) and Linear Dynamic Range (LDR) of Developed and Reported Fluorescence-based Caspase-3 Sensors

analytical method	limit of detection (LOD)	linear dynamic range (LDR)	reference
FRET (AuNP and QD)	394 pg/mL	394−4130 pg/mL	Li et al. *ACS Appl. Mater. Interfaces* **2013**, *19*, 9798−9802[43]
FRET (GO and FAM)	7.25 ng/mL	7.25−362 ng/mL	Wang et al. *Angew. Chem. Int. Ed.* **2011**, *123*, 7203−7207[44]
FRET (dabcyl and FAM)	1.12 ng/mL	1.12−4.8 ng/mL	Li et al. *Chem. Commun.* **2015**, *51*, 14520−14523[45]
photoelectrochemical sensor	0.14 ng/mL	0.2−20 ng/mL	Yang et al. *Chem. Commun.* **2018**, *54*, 4830−4833[46]
FRET (tryptophan and coumarin derivatives)	44.5 ng/mL	not reported	Kang et al. *Biosens. Bioelectron.* **2015**, *67*, 413−418[47]
FRET (MoS_2 and FAM)	0.33 ng/mL	2−360 ng/mL	Li et al. *J. Colloid Interface Sci.* **2019**, *543*, 96−105[48]
FRET (iridium(111) and rhodamine)	not reported (intracellular analysis only)	not reported (intracellular analysis only)	Wu et al. *J. Am. Chem. Soc.* **2020**, *142*, 1057−1064[49]
MEF (AuNP and FITC)	10 pg/mL	0.01−10 ng/mL	This work

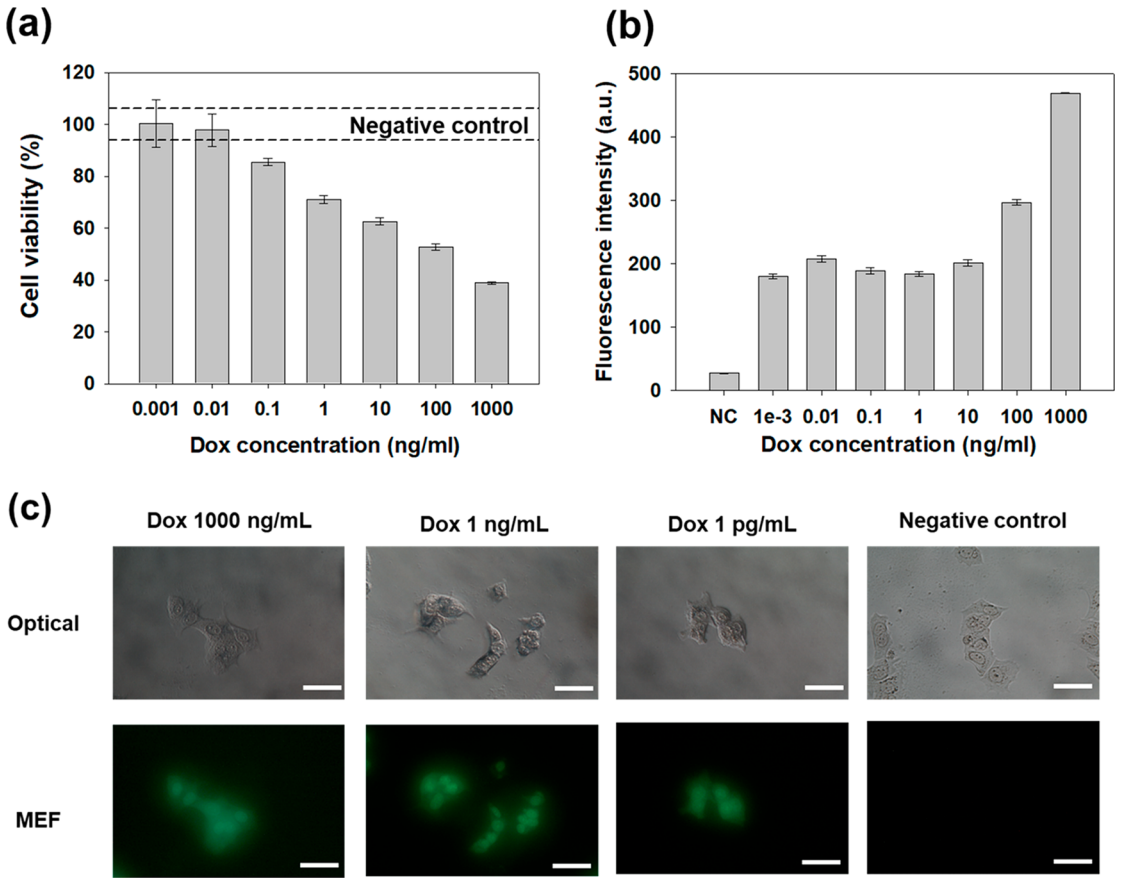

Figure 4. Apoptotic cell detection using the MEF-based bifunctional AuNP biosensor. (a) MTT assay of the MCF-7 along with the Dox concentration from 0.001 to 1000 ng/mL. (b) Fluorescence intensity of the bifunctional AuNP-internalized MCF-7 cell after Dox treatment from 0.001 to 1000 ng/mL, corresponding to panel a. (c) Fluorescence images of the Dox-treated MCF-7 cells. Scale bars are 100 μm.

fluorescence when caspase-3 degraded the peptide bridge because ssDNA could keep the optimal distance for generating MEF. To compare the fluorescence signal by the caspase-3 reaction without ssDNA, caspase-3 was applied to the bifunctional AuNPs with and without ssDNA. In the case of the AuNP−peptide−FITC without ssDNA, the fluorescence signal changed because of the caspase-3 reaction, ranging from 55 to 115 (a.u.). This was caused by the fluorescence quenching−dequenching effect (Figure 3a). On the contrary, novel MEF-based Au nanosensors showed a significant increase in the fluorescence intensity (up to 3000 au) when caspase-3 degraded the specific peptide sequence (Figure 3b). A comparison of the fluorescence intensity of the 10 ng/mL caspase-3 reaction in the absence and presence of ssDNA showed a ∼25-fold difference. For the testing of sensitivity performance, caspase-3 was applied in a 10 ng/mL to a 78 pg/mL concentration range. In the case of using the dequenching effect, caspase-3 below 5 ng/mL could not be detected by the typical quenching−dequenching system (Figure 3a). In contrast, caspase-3 was successfully measured within the testing concentration range in the case of the MEF-inducing bifunctional AuNPs with ssDNA (Figure 3b). With a signal

https://dx.doi.org/10.1021/acs.nanolett.0c02343
Nano Lett. XXXX, XXX, XXX−XXX

intensity of 78 pg/mL, it still showed a big difference in the negative control (quenching state). For the identification of the sensitivity and detection range of the Au nanosensor, fluorescence intensities were measured by the caspase-3 concentration, half-dilution from 10 ng/mL to 5 pg/mL. As shown in Figure 3c,d, caspase-3 was successfully detected from 10 pg/mL to 10 ng/mL with a high R^2 value (>0.98). In the case of 5 pg/mL, the fluorescence signal was similar to that of the negative control. In comparison with the typical quenching−dequenching system in Figure 3a, the MEF effect could improve the sensitivity of the AuNP-based sensing system. In addition, both the limit of detection (LOD) and the linear dynamic range are superior to those of other previously published fluorescence-based caspase-3 biosensing systems (Table 1). In addition, the real-time fluorescence response could be measured over time by using this system (Figure 3e). The fluorescence intensity gradually increased by reaction time with caspase-3 and was saturated from 60 to 70 min due to the finite amount of peptide attached on the AuNP surface.

For the verification of selectivity using this biosensing system, diverse proteolytic enzymes and a caspase-3 inhibitor with caspase-3 were applied to the DEVD-functionalized bifunctional AuNP (Supplementary Figure 4). As exhibited, caspase-1 and PSA had little effect on the fluorescence regeneration because they could not degrade the peptide strand. In the case of the caspase-3 inhibitor with caspase-3, the fluorescence signal was not generated due to the inhibition of the peptide cleavage by caspase-3. These results clearly indicated that it could work only with caspase-3-mediated peptide degradation. On the contrary, this sensing system can be applied to detect other proteolytic enzymes by changing the cleavable peptide sequences. In Supplementary Figure 5, MMP-2 and caspase-1 were tested to generate a fluorescence signal by AuNPs with their specific cleavage sequences (PLGVR and YVAD). Comparing the negative control, which was in a quenching state, MMP-2 and caspase-1 also induced strong fluorescence signals by successfully degrading specific peptide sequences.

Caspase-3-related Apoptotic Cell Detection Based on MEF-Induced Bifunctional AuNP. Apoptosis, or programmed cell death, has been a concern in many human diseases such as cancers and neurodegenerative diseases.[42] In the apoptotic cells, caspase-3 is proteolytically activated by the cleavage of pro-caspase-3 by caspase-8 and degrades several intracellular proteins to proceed the apoptosis. Therefore, a caspase-3-mediated apoptotic cell detection system has been developed using the FRET-based technique composed of the donor (fluorescent dye), quencher, and DEVD-including peptide. The proposed MEF-based fluorescence sensing system is a one-step, simple detection strategy and is superior to the FRET-based system regarding the sensitivity with sharing the same peptide cleavage reaction mechanism. In Figure 4 and Supplementary Figure 6, doxorubicin (Dox)-induced apoptotic cells were examined to show the intracellular caspase-3 activation by the bifunctional AuNP. Comparing the cell viability with the MEF, a 3-(4,5-dimethylthiazol-2-yl)-2,5-diphenyltetrazolium bromide (MTT) assay was conducted according to the concentration of the Dox. The cell viability exhibited the inverse linear relationship to the Dox concentration from 0.1 to 1000 ng/mL. However, the linearity was not shown below 0.1 ng/mL because the Dox quantity was too low to affect the cell viability via the MTT assay (Figure 4a). On the contrary, fluorescence regeneration could be easily observed below 0.1 ng/mL of Dox concentration due to its highly sensitive detection of caspase-3 (Figure 4b). In Figure 4c, the fluorescence signal could also be confirmed by fluorescence images, as the cell viability was not affected by the Dox toxical effect. Using this phenomenon, minor impacts against some toxic materials, which could induce apoptosis, can be identified by the MEF-induced AuNP in advance. Because the bifunctional AuNPs could not affect the cell viability with strong fluorescence emission by the intracellular caspase-3, real-time monitoring of the intracellular proteolytic enzymes in a live cell could be achieved. For the verification of real-time monitoring of the preapoptotic cell, fluorescence images of bifunctional AuNP-treated preapoptotic MCF-7 cells are exhibited in Supplementary Figure 7. Fluorescence emission could be observed for 60 min by treatment with 1 pg/mL Dox without any destructive methods, such as immunostaining or other cell fixation solution.

CONCLUSIONS

In summary, caspase-3, which is a representative proteolytic enzyme and diagnostic marker of several diseases, was simply (one-step proteolytic reaction) and rapidly (<1 h) detected using a bifunctional AuNP by inducing MEF phenomena. Notably, it exhibited highly sensitive detection as low as a femtomolar concentration in a cell-free configuration, ranging from 10 to 10 000 pg/mL. This MEF-based primarily proof-of-concept approach for the detection of several proteolytic enzymes such as MMPs and the caspase family provides the framework for the development of highly sensitive biosensors by changing cleavable peptide sequences. It is superior to the FRET-based sensors with respect to sensitive detection, which was provided by the signal enhancement effect of the MEF by caspase-3 in a rapid and simple manner. Furthermore, it could be applied to detect preapoptotic cells by the cellular internalization of bifunctional AuNPs, even if the cell viability is not yet affected by the cytotoxic material. Because caspase-3 is considered as one of potential hallmarks of cancer, this nanosensor could be further applied to the diagnosis of ultrasmall or metastatic tumors *in vivo*. We propose that this approach is simpler, faster, and more cost-effective than conventional immunoassay approaches and that it can be widely applied for the early diagnosis of cancer and neurodegenerative diseases by measuring any proteolytic enzyme biomarker.

ASSOCIATED CONTENT

Supporting Information

The Supporting Information is available free of charge at https://pubs.acs.org/doi/10.1021/acs.nanolett.0c02343.

Materials and methods. Supplementary Figure 1. Characterization of the bifunctional AuNP. Supplementary Figure 2. Confirmation of the peptide and ssDNA-functionalized Au nanoparticle. Supplementary Figure 3. Fluorescence signal intensities by the concentration of bifunctional AuNPs. Supplementary Figure 4. Fluorescence intensity at 520 nm of the caspase-1, PSA, caspase-3, and caspase-3 with its inhibitor. Supplementary Figure 5. Fluorescence intensity at 520 nm for the measurement of other proteolytic enzymes by using the MEF nanosensor system with target-specific peptide sequences. Supplementary Figure 6. Larger scale fluorescence images of the Dox-treated (1 pg/mL) MCF-7 cells than

https://dx.doi.org/10.1021/acs.nanolett.0c02343
Nano Lett. XXXX, XXX, XXX−XXX

Figure 4c with internalization of bifunctional AuNPs. Supplementary Figure 7. Real-time fluorescence images of the MCF-7 cells with the internalization of bifunctional AuNPs after 10, 20, 30, 40, 50, and 60 min of dosing Dox (1 pg/mL) (PDF)

AUTHOR INFORMATION

Corresponding Author

Jeong-Woo Choi − *Department of Chemical & Biomolecular Engineering, Sogang University, Seoul 04107, Republic of Korea;* orcid.org/0000-0003-0100-0582; Email: jwchoi@sogang.ac.kr; http://nbel.sogang.ac.kr/nbel/index.html

Author

Jin-Ha Choi − *Department of Chemical & Biomolecular Engineering, Sogang University, Seoul 04107, Republic of Korea;* orcid.org/0000-0002-1632-9586

Complete contact information is available at: https://pubs.acs.org/10.1021/acs.nanolett.0c02343

Author Contributions

J.-H.C. and J.-W.C. designed the original idea. J.-H.C. conducted the experiments. J.-H.C. wrote the manuscript.

Notes

The authors declare no competing financial interest.

ACKNOWLEDGMENTS

This research was supported by the Basic Science Research Program through the National Research Foundation of Korea (NRF) funded by the Ministry of Education (No.2019R1A2C3002300), and Basic Science Research Program through the National Research Foundation of Korea (NRF) funded by the Ministry of Education (No.2016R1A6A1A03012845), and the Basic Science Research Program through the National Research Foundation of Korea (NRF) funded by the Ministry of Education (No.2018R1A6A3A11051465).

ABBREVIATIONS

MEF, metal-enhanced fluorescence
AuNP, Au nanoparticle
FITC, fluorescein isothiocyanate
MMP, matrix metalloproteinase
PSA, prostate-specific antigens
FRET, fluorescence resonance energy transfer
LSPR, localized surface plasmon resonance
ssDNA, single-stranded DNA

REFERENCES

(1) Burger, M. M. Proteolytic enzymes initiating cell division and escape from contact inhibition of growth. *Nature* **1970**, *227*, 170−1.
(2) Neurath, H.; Walsh, K. A. Role of proteolytic enzymes in biological regulation (a review). *Proc. Natl. Acad. Sci. U. S. A.* **1976**, *73*, 3825−32.
(3) Egeblad, M.; Werb, Z. New functions for the matrix metalloproteinases in cancer progression. *Nat. Rev. Cancer* **2002**, *2*, 161−74.
(4) Parks, W. C.; Wilson, C. L.; Lopez-Boado, Y. S. Matrix metalloproteinases as modulators of inflammation and innate immunity. *Nat. Rev. Immunol.* **2004**, *4*, 617−629.
(5) Visse, R.; Nagase, H. Matrix metalloproteinases and tissue inhibitors of metalloproteinases: structure, function, and biochemistry. *Circ. Res.* **2003**, *92*, 827−39.
(6) Deryugina, E. I.; Quigley, J. P. Matrix metalloproteinases and tumor metastasis. *Cancer Metastasis Rev.* **2006**, *25*, 9−34.
(7) Navya, P. N.; Kaphle, A.; Srinivas, S. P.; Bhargava, S. K.; Rotello, V. M.; Daima, H. K. Current trends and challenges in cancer management and therapy using designer nanomaterials. *Nano Converg* **2019**, *6*, 23.
(8) Sweeney, M. D.; Sagare, A. P.; Zlokovic, B. V. Blood−brain barrier breakdown in Alzheimer disease and other neurodegenerative disorders. *Nat. Rev. Neurol.* **2018**, *14*, 133.
(9) Galliera, E.; Tacchini, L.; Corsi Romanelli, M. M. Matrix metalloproteinases as biomarkers of disease: updates and new insights. *Clin. Chem. Lab. Med.* **2015**, *53*, 349−355.
(10) Chang, K.-H.; Wu, Y.-R.; Chen, Y.-C.; Chen, C.-M. Plasma inflammatory biomarkers for Huntington's disease patients and mouse model. *Brain, Behav., Immun.* **2015**, *44*, 121−127.
(11) Huang, J.; Li, J.; Lyu, Y.; Miao, Q.; Pu, K. Molecular optical imaging probes for early diagnosis of drug-induced acute kidney injury. *Nat. Mater.* **2019**, *18*, 1133.
(12) Cheng, P.; Miao, Q.; Li, J.; Huang, J.; Xie, C.; Pu, K. Unimolecular chemo-fluoro-luminescent reporter for crosstalk-free duplex imaging of hepatotoxicity. *J. Am. Chem. Soc.* **2019**, *141*, 10581−10584.
(13) Choi, J.-H.; Kim, H.; Choi, J.-H.; Choi, J.-W.; Oh, B.-K. Signal enhancement of silicon nanowire-based biosensor for detection of matrix metalloproteinase-2 using DNA-Au nanoparticle complexes. *ACS Appl. Mater. Interfaces* **2013**, *5*, 12023−12028.
(14) Choi, J.-H.; Kim, H.; Kim, H.-S.; Um, S. H.; Choi, J.-W.; Oh, B.-K. MMP-2 detective silicon nanowire biosensor using enzymatic cleavage reaction. *J. Biomed. Nanotechnol.* **2013**, *9*, 732−735.
(15) Lee, J.; Yun, J. Y.; Lee, W. C.; Choi, S.; Lim, J.; Jeong, H.; Shin, D.-S.; Park, Y. J. A reference electrode-free electrochemical biosensor for detecting MMP-9 using a concentric electrode device. *Sens. Actuators, B* **2017**, *240*, 735−741.
(16) Yang, Y.; Liang, Y.; Zhang, C.-y. Label-free and homogenous detection of caspase-3-like proteases by disrupting homodimerization-directed bipartite tetracysteine display. *Anal. Chem.* **2017**, *89*, 4055−4061.
(17) Yang, R.; Li, Y.; Zou, K.; Meng, L.; Zhang, X.; Chen, J. A label-free and blocker-free photoelectrochemical strategy for highly sensitive caspase-3 assay. *Chem. Commun.* **2018**, *54*, 4830−4833.
(18) Murai, S.; Yamaguchi, Y.; Shirasaki, Y.; Yamagishi, M.; Shindo, R.; Hildebrand, J. M.; Miura, R.; Nakabayashi, O.; Totsuka, M.; Tomida, T.; et al. A FRET biosensor for necroptosis uncovers two different modes of the release of DAMPs. *Nat. Commun.* **2018**, *9*, 4457.
(19) Choi, J. H.; Kim, H. S.; Choi, J.-W.; Hong, J. W.; Kim, Y.-K.; Oh, B.-K. A novel Au-nanoparticle biosensor for the rapid and simple detection of PSA using a sequence-specific peptide cleavage reaction. *Biosens. Bioelectron.* **2013**, *49*, 415−419.
(20) Xie, S.; Zhang, J.; Yuan, Y.; Chai, Y.; Yuan, R. An electrochemical peptide cleavage-based biosensor for prostate specific antigen detection via host−guest interaction between ferrocene and β-cyclodextrin. *Chem. Commun.* **2015**, *51*, 3387−3390.
(21) Xia, N.; Deng, D.; Wang, Y.; Fang, C.; Li, S.-J. gold nanoparticle-based colorimetric method for the detection of prostate-specific antigen. *Int. J. Nanomed.* **2018**, *13*, 2521.
(22) Melnychuk, N.; Klymchenko, A. S. DNA-functionalized dye-loaded polymeric nanoparticles: ultrabright FRET platform for amplified detection of nucleic acids. *J. Am. Chem. Soc.* **2018**, *140*, 10856−10865.
(23) Morales-Narváez, E.; Merkoçi, A. Graphene oxide as an optical biosensing platform. *Adv. Mater.* **2012**, *24*, 3298−3308.
(24) Zhang, Q.; Zhang, D.; Xu, G.; Xu, Y.; Lu, Y.; Li, S.; Liu, Q. Spectroscopic detection of thrombin with peptides self-assembled on gold nanoparticles hybridized graphene oxide. *Sens. Actuators, B* **2017**, *242*, 443−449.
(25) Wang, D.; Chai, Y.; Yuan, Y.; Yuan, R. A Peptide Cleavage-Based Ultrasensitive Electrochemical Biosensor with an Ingenious

https://dx.doi.org/10.1021/acs.nanolett.0c02343
Nano Lett. XXXX, XXX, XXX−XXX

Two-Stage DNA Template for Highly Efficient DNA Exponential Amplification. *Anal. Chem.* **2017**, *89*, 8951−8956.
(26) Zheng, Y.; Ma, Z. Dual-reaction triggered sensitivity amplification for ultrasensitive peptide-cleavage based electrochemical detection of matrix metalloproteinase-7. *Biosens. Bioelectron.* **2018**, *108*, 46−52.
(27) Herpoldt, K.-L.; Artzy-Schnirman, A.; Christofferson, A. J.; Makarucha, A. J.; de la Rica, R.; Yarovsky, I.; Stevens, M. M. Designing fluorescent peptide sensors with dual specificity for the detection of HIV-1 protease. *Chem. Mater.* **2015**, *27*, 7187−7195.
(28) Nguyen, P.-D.; Cong, V. T.; Baek, C.; Min, J. Fabrication of peptide stabilized fluorescent gold nanocluster/graphene oxide nanocomplex and its application in turn-on detection of metalloproteinase-9. *Biosens. Bioelectron.* **2017**, *89*, 666−672.
(29) Chen, W.-H.; Luo, G.-F.; Xu, X.-D.; Jia, H.-Z.; Lei, Q.; Han, K.; Zhang, X.-Z. Cancer-targeted functional gold nanoparticles for apoptosis induction and real-time imaging based on FRET. *Nanoscale* **2014**, *6*, 9531−9535.
(30) Chen, H.; Fang, A.; Zhang, Y.; Yao, S. Silver triangular nanoplates as an high efficiently FRET donor-acceptor of upconversion nanoparticles for ultrasensitive "Turn on-off" protamine and trypsin sensor. *Talanta* **2017**, *174*, 148−155.
(31) Wu, M.; Petryayeva, E.; Algar, W. R. Quantum dot-based concentric FRET configuration for the parallel detection of protease activity and concentration. *Anal. Chem.* **2014**, *86*, 11181−11188.
(32) Wu, M.; Wang, X.; Wang, K.; Guo, Z. An ultrasensitive fluorescent nanosensor for trypsin based on upconversion nanoparticles. *Talanta* **2017**, *174*, 797−802.
(33) Jeong, Y.; Kook, Y.-M.; Lee, K.; Koh, W.-G. Metal enhanced fluorescence (MEF) for biosensors: General approaches and a review of recent developments. *Biosens. Bioelectron.* **2018**, *111*, 102−116.
(34) Li, M.; Cushing, S. K.; Wu, N. Plasmon-enhanced optical sensors: a review. *Analyst* **2015**, *140*, 386−406.
(35) Lee, T.; Jang, J.; Jeong, H.; Rho, J. Plasmonic- and dielectric-based structural coloring: from fundamentals to practical applications. *Nano Converg* **2018**, *5*, 1−21.
(36) Lee, J. H.; Choi, J. H.; Chueng, S. T. D.; Pongkulapa, T.; Yang, L.; Cho, H. Y.; Choi, J. W.; Lee, K. B. Nondestructive characterization of stem cell neurogenesis by a magneto-plasmonic nanomaterial-based exosomal mirna detection. *ACS Nano* **2019**, *13*, 8793.
(37) Choi, J. H.; Lim, J.; Shin, M.; Choi, J. W. CRISPR/Cas12a-based Cell-Free DNA Biosensor via Au nanoparticle-assisted Metal-Enhanced Fluorescence and Colorimetric methods without Nucleic Acid Amplification. *Journal Name* **2020**, submitted.
(38) Buschhaus, J.; Humphries, B.; Luker, K.; Luker, G. A Caspase-3 Reporter for Fluorescence Lifetime Imaging of Single-Cell Apoptosis. *Cells* **2018**, *7*, 57.
(39) Feng, A. L.; You, M. L.; Tian, L.; Singamaneni, S.; Liu, M.; Duan, Z.; Lu, T. J.; Xu, F.; Lin, M. Distance-dependent plasmon-enhanced fluorescence of upconversion nanoparticles using polyelectrolyte multilayers as tunable spacers. *Sci. Rep.* **2015**, *5*, 7779.
(40) Delfino, I.; Cannistraro, S. Optical investigation of the electron transfer protein azurin−gold nanoparticle system. *Biophys. Chem.* **2009**, *139*, 1−7.
(41) Li, L.; Mu, Q.; Zhang, B.; Yan, B. Analytical strategies for detecting nanoparticle−protein interactions. *Analyst* **2010**, *135*, 1519−1530.
(42) Budihardjo, I.; Oliver, H.; Lutter, M.; Luo, X.; Wang, X. Biochemical pathways of caspase activation during apoptosis. *Annu. Rev. Cell Dev. Biol.* **1999**, *15*, 269−290.
(43) Li, J.; Li, X.; Shi, X.; He, X.; Wei, W.; Ma, N.; Chen, H. Highly sensitive detection of caspase-3 activities via a nonconjugated gold nanoparticle−quantum dot pair mediated by an inner-filter effect. *ACS Appl. Mater. Interfaces* **2013**, *5*, 9798−9802.
(44) Wang, H.; Zhang, Q.; Chu, X.; Chen, T.; Ge, J.; Yu, R. Graphene oxide−peptide conjugate as an intracellular protease sensor for caspase-3 activation imaging in live cells. *Angew. Chem., Int. Ed.* **2011**, *50*, 7065−7069.
(45) Li, S. Y.; Liu, L. H.; Cheng, H.; Li, B.; Qiu, W. X.; Zhang, X. Z. A dual-FRET-based fluorescence probe for the sequential detection of MMP-2 and caspase-3. *Chem. Commun.* **2015**, *51*, 14520−14523.
(46) Yang, R.; Li, Y.; Zou, K.; Meng, L.; Zhang, X.; Chen, J. A label-free and blocker-free photoelectrochemical strategy for highly sensitive caspase-3 assay. *Chem. Commun.* **2018**, *54*, 4830−4833.
(47) Kang, H. J.; Kim, J. H.; Chung, S. J. Homogeneous detection of caspase-3 using intrinsic fluorescence resonance energy transfer (iFRET). *Biosens. Bioelectron.* **2015**, *67*, 413−418.
(48) Li, X.; Li, Y.; Qiu, Q.; Wen, Q.; Zhang, Q.; Yang, W.; Yuwen, L.; Weng, L.; Wang, L. Efficient biofunctionalization of MoS_2 nanosheets with peptides as intracellular fluorescent biosensor for sensitive detection of caspase-3 activity. *J. Colloid Interface Sci.* **2019**, *543*, 96−105.
(49) Wu, Q.; Zhang, K. Y.; Dai, P.; Zhu, H.; Wang, Y.; Song, L.; Wang, L.; Liu, S.; Zhao, Q.; Huang, W. Bioorthogonal "Labeling after Recognition" Affording an FRET-based Luminescent Probe for Detecting and Imaging Caspase-3 via Photoluminescence Lifetime Imaging. *J. Am. Chem. Soc.* **2020**, *142*, 1057−1064.

https://dx.doi.org/10.1021/acs.nanolett.0c02343
Nano Lett. XXXX, XXX, XXX−XXX